Stability of the Darwinian Dynamics

Effect of Intraspecific Competition and Human Intervention

Satouri, Mohammadreza; Rezaei, Jafar; Staňková, Kateřina

DOI
10.1007/s13235-025-00629-3

Publication date
2025

Document Version
Final published version

Published in
Dynamic Games and Applications

Dynamic Games and Applications
https://doi.org/10.1007/s13235-025-00629-3

Stability of the Darwinian Dynamics: Effect of Intraspecific Competition and Human Intervention

Mohammadreza Satouri[1] · **Jafar Rezaei**[1] · **Kateřina Staňková**[1]

Accepted: 10 February 2025

Abstract
We analyze the stability of a game-theoretic model of a polymorphic eco-evolutionary system in the presence of human intervention. The goal is to understand how the intensity of this human intervention and competition within the system impact its stability, with cancer treatment as a case study. In this case study, the physician applies anti-cancer treatment, while cancer, consisting of treatment-sensitive and treatment-resistant cancer cells, responds by evolving more or less treatment-induced resistance, according to Darwinian evolution. We analyze how the existence and stability of the cancer eco-evolutionary equilibria depend on the treatment dose and rate of competition between cancer cells of the two different types. We also identify initial conditions for which the resistance grows unbounded. In addition, we adopt the level-set method to find viscosity solutions of the corresponding Hamilton–Jacobi equation to estimate the basins of attraction of the found eco-evolutionary equilibria and simulate typical eco-evolutionary dynamics of cancer within and outside these estimated basins. While we illustrate our results on the cancer treatment case study, they can be generalized to any situation where a human aims at containing, eradicating, or saving Darwinian systems, such as in managing antimicrobial resistance, fisheries management, and pest management. The obtained results help our understanding of the impact of human interventions and intraspecific competition on the possibility of containing, eradicating, or saving evolving species. This will help us with our ability to control such systems.

Keywords Evolutionary game theory · Eco-evolutionary dynamics · Darwinian dynamics · Stability · Mathematical oncology

✉ Mohammadreza Satouri
m.satouri@tudelft.nl

Jafar Rezaei
j.rezaei@tudelft.nl

Kateřina Staňková
k.stankova@tudelft.nl

[1] Faculty of Technology, Policy and Management, Institute for Health Systems Science, Delft University of Technology, Delft, The Netherlands

Published online: 20 March 2025

1 Introduction

Human actions often lead to a rapid evolution in biological entities that humans want to save, contain, or eradicate [1–3]. This rapid evolution may lead these systems to states that are unintended or undesirable. For example, an attempt to eradicate the diamondback moth using different types of insecticides has led to its development of resistance to about 100 active chemicals, putting the diamondback moth first among the 20 most insecticide-resistant insect species [4]. In general, pest resistance as a consequence of the abundant application of pesticides is a well-recognized problem worldwide [5–8]. Similarly, we observe an antibiotic resistance crisis as a consequence of a too extensive antibiotic application [9], decreased fish size followed by a collapse of fisheries due to overfishing [10, 11], and treatment-induced resistance of cancer cells in response to the application of high-dose anticancer treatments [12–17]. In all these examples, human interventions drive the evolution of traits that are undesirable to humans [18–20].

Mathematical models, such as those within evolutionary game theory, can help us understand how different selection pressures imposed by humans affect the evolution of biological systems in terms of their eco-evolutionary dynamics [21–25]. When humans impose their actions on the evolving systems, they become Stackelberg leaders in a game against or for nature. The Stackelberg evolutionary game theory combines Stackelberg and evolutionary game theory and has recently been termed the Stackelberg evolutionary game [19, 20].

While Stackelberg evolutionary game theory focuses on human actions that maximize human own benefit when interacting with evolutionary followers, much less attention has been given to studying how competition between evolutionary followers contributes to human's ability to bring eco-evolutionary dynamics of these followers to states desired by the human. Here, we will bridge this gap by studying the impact of both the rate of competition between different types of evolutionary followers and the intensity of human action on their ability to stabilize the followers' eco-evolutionary dynamics.

As a specific case study, we will consider cancer treatment, where the physician applies a constant treatment dose to target a polymorphic cancer cell population consisting of treatment-sensitive and treatment-resistant cancer cells. These cells compete with each other for space and resources, to proliferate and survive [26, 27]. In our modeling, this competition is captured through the carrying capacity and competition matrix, leading to the density- and frequency-dependent selection in cancer cells, respectively.

The resistant cancer cells may evolve more or less resistance in response to both the treatment dose and rate of competition within the cancer cell population. While in early-stage cancer the evolution of resistance may not occur when no resistant cells are present a priori and/or when they are outcompeted by sensitive cells, here we consider a case of advanced cancer where the evolution of resistance is typically inevitable. [28–30]. Our model combines qualitative and quantitative resistance [23]. While we have a distinct resistant population, this population does not have a fixed treatment-induced resistance. Rather, this resistance evolves as a quantitative trait, affected by both the pre-existing and treatment-induced resistant cells.

Our game-theoretic model of cancer treatment is an extension of the evolutionary model introduced by Pressley et al. [31]. Our model incorporates competition between cancer cells to study the impact of competition between cancer cells and the administered treatment dose on the ability to stabilize cancer dynamics.

The rest of this paper is organized as follows: we first introduce our Darwinian dynamics model, which accounts for the effects of both human intervention and intraspecific competition (Sect. 2). Next, we describe the methodology for analyzing equilibria and their stability,

estimating basins of attraction, and simulating typical cancer eco-evolutionary trajectories (Sect. 3). We then present the results regarding stability, basins of attraction, and cancer trajectories (Sect. 4). Finally, we discuss the implications of our findings for mathematical oncology and game theory, address limitations, and suggest future research directions (Sect. 5).

2 Game-theoretic model

Let us consider a polymorphic eco-evolutionary system modeled through Darwinian dynamics [32–34] where a human imposes selection pressure on this system through a constant action $m \in \mathbb{R}^0_+ = \mathbb{R}_+ \cup \{0\}$. Here, we are interested in how cancer eco-evolutionary equilibria depend on the treatment dose m and competition coefficients α_{ij}. For this reason, we do not assume *a priori* any dependence of m on state variables in our model. In general, treatment can be time-varying. However, because of our focus on the equilibria, we assume the treatment dose to be constant. The method we use allows for extending this framework to piecewise constant treatment doses.

The population and evolving trait of individuals of type i will be denoted by x_i and u_i, respectively, where $\mathbf{x}(t) = (x_i(t))$ and $\mathbf{u}(t) = (u_i(t))$ define population and evolving traits of all individuals at time t.

Ecological dynamics of individuals of type i are defined as

$$\dot{x}_i(t) = x_i(t) G(v(t), \mathbf{u}(t), \mathbf{x}(t), m)\big|_{v(t)=u_i(t)} \tag{1}$$

where G refers to the fitness-generating function from Darwinian dynamics [32] and $v(t)$ is the trait of a focal individual of type i at time t.

Following Fisher's fundamental theorem of natural selection, the focal evolutionary trait $v(t)$ changes in the direction of the fitness gradient $\frac{\partial G}{\partial v}$ [35]. The evolutionary dynamics are defined as follows:

$$\dot{u}_i(t) = \sigma_i \frac{\partial G(v(t), \mathbf{u}(t), \mathbf{x}(t), m)}{\partial v(t)}\bigg|_{v(t)=u_i(t)} \tag{2}$$

The rate at which the trait $u_i(t)$ changes is given by an evolutionary speed σ_i. A measure of how quickly the trait responds to selection gradients, σ_i, encapsulates the combined effects of genetic variation, mutation rates, and the overall responsiveness of the trait to evolutionary pressures [32]. While this could reflect the trait's sensitivity to spontaneous genetic changes, in our formulation, σ_i is treated as a constant. It thus serves as an aggregate measure of evolutionary responsiveness, encompassing interactions between the trait and the rest of the system dynamics.

In our model, we assume that all individuals' strategies have the same evolutionary speed, while in reality σ_i's may depend on other parameters, such as the population size $\mathbf{x}$ and/or may be different for different types of individuals [36–38]. Moreover, as long as σ_i is constant, it does not affect the eco-evolutionary equilibria of the system.

While the eco-evolutionary dynamics (1–2) can define any polymorphic Darwinian system responding to a constant leader's action m, here we will analyze an example of cancer treatment game. In this example, $m \geq 0$ corresponds to a constant treatment dose applied by a physician and $\mathbf{x}(t) = (x_S(t), x_R(t))^\top$ is a vector of populations of cancer cells that are sensitive (S) and resistant (R) to the treatment, respectively, at time t.

Table 1 Description of variables and parameters utilized in (4), including their values/ranges

Variable/parameters	Description	Value/range
$\mathbf{x} = \begin{pmatrix} x_S \\ x_R \end{pmatrix}$	Population of cancer cells	$[0, K]^2$
u_S	Resistance strategy of sensitive cells	0
u_R	Resistance strategy of resistant cells	$\mathbb{R}_0^+$
v	Resistance strategy of a focal resistant cell	$\mathbb{R}_0^+$
g	Magnitude of cost of resistance	$\mathbb{R}_0^+$
K	Carrying capacity	$\mathbb{R}_0^+$
α_{ij}	Competition coefficient	$\mathbb{R}_0^+$
σ	Evolutionary speed	$\mathbb{R}_0^+$
k	Innate resistance	$[1, +\infty]$
b	Magnitude of resistance benefit	$\mathbb{R}_0^+$
m	Treatment	$\mathbb{R}_0^+$
$r_{\max}$	Maximum growth rate	$\mathbb{R}_0^+$
d	Natural death rate	$\mathbb{R}_0^+$

We assume that only resistant cells have the capacity to evolve resistance $u_R(t) \in \mathbb{R}_+^0$ and that the G-function of these cells has the same form as introduced in [20, 31], i.e.,

$$G(v(t), \mathbf{u}(t), \mathbf{x}(t), m) = r(v(t)) \left(1 - \frac{\sum_{j\in\{R,S\}} a(v(t), u_j(t))x_j(t)}{K}\right) - d - \frac{m}{k + bv(t)} \tag{3}$$

with $a(u_i, u_j) = \alpha_{ij}$ defining a competition effect of type j on type i, where $i, j \in \{R, S\}$. In (3), the efficacy of the drug is reduced by a focal cell's resistance $v(t)$, innate drug immunity k, and the benefit b of the resistance $v(t)$ in reducing therapy efficacy. Various in-vitro and in-vivo studies have demonstrated that resistance may incur a cost [39–41]. Therefore, our model includes this cost of resistance, which affects the proliferation rate of resistant cells. We assume that the resistance cost is expressed through the growth rate $r(v(t))$ of resistant cells, which decreases with increasing resistance, i.e., $r(v(t)) = r_{\max}\, e^{-g\, v(t)}$.

In our model, sensitive cells cannot evolve resistance, i.e., $u_S(t) = 0$ for all t.

In the remainder of this paper, we drop the time symbol t for the sake of simplicity and readability of our notation.

The model of cancer eco-evolutionary dynamics then reads as follows:

$$\begin{aligned}
\dot{x}_S &= x_S \left(r_{\max}\left(1 - \frac{\alpha_{SS}x_S + \alpha_{SR}x_R}{K}\right) - d - \frac{m}{k}\right) \\
\dot{x}_R &= x_R \left(r_{\max}e^{-g\,u_R}\left(1 - \frac{\alpha_{RS}x_S + \alpha_{RR}x_R}{K}\right) - d - \frac{m}{k + b\,u_R}\right) \\
\dot{u}_R &= \sigma \left(-g r_{\max}e^{-g u_R}\left(1 - \frac{\alpha_{RR}x_R + \alpha_{RS}x_S}{K}\right) + \frac{bm}{(k + bu_R)^2}\right)
\end{aligned} \tag{4}$$

The variables and parameters utilized in (4) and their ranges are summarized in Table 1

3 Methods

3.1 Stability analysis of eco-evolutionary equilibria

We analyze the stability of eco-evolutionary equilibria of (4) using the Lyapunov indirect method [42]. This entails linearizing the eco-evolutionary dynamics (4) around its equilibria and calculating the eigenvalues of the corresponding Jacobian matrix at those equilibria. If real parts of all eigenvalues of the Jacobian expressed in a given equilibrium are negative, this equilibrium is locally stable. If at least one eigenvalue has a positive real part, the corresponding equilibrium is unstable.

3.2 Estimating basins of attraction

In this study, we adopt the parameter values K, k, σ, and b as suggested by [31]. The remaining parameters are selected to showcase the full spectrum of equilibria and their stability outcomes for the dynamics described in (4). We summarize all parameters in Table 2.

When there is a single locally stable equilibrium for the dynamics (4), we estimate its basin of attraction using the level set method [43], following the approach described by Yuan and Li [44]. We rescale the initial conditions to $(x_S(0)/K, x_R(0)/K, u_R(0))$, so that they are within the range $[0, 1] \times [0, 1] \times [0, 8]$, with other parameter values set as listed in Table 2.[1]

We partition the state space $[0, 1] \times [0, 1] \times [0, 8]$ into a computational grid with a step size of 0.05, to facilitate numerical calculations. Using this grid, we compute viscosity solutions for the corresponding Hamilton-Jacobi equation by solving it backward in time as described in [44]. To achieve this, we employ Ian Mitchell's toolbox for level set methods [45] since it is capable of solving time-dependent Hamilton-Jacobi equations in any dimension.

When multiple locally stable equilibria are present, we estimate their basins of attraction within the state space $[0, 1] \times [0, 1] \times [0, 8]$. To achieve this, we randomly select 10000 initial conditions $(x_S(0)/K, x_R(0)/K, u_R(0))$ within this state space and simulate their eco-evolutionary trajectories.

If a trajectory converges to a stable equilibrium, the initial condition is considered within the basin of attraction of that equilibrium. Conversely, if during a simulation u_R grows unbounded, it indicates that the initial condition is outside the basin of attraction of the considered stable equilibrium, highlighting regions where the system dynamics lead to instability.

In simulations, we consider three different cases. Case 1 with one locally stable trivial equilibrium, case 2 with one locally stable interior equilibrium, and case 3 with two locally stable fully sensitive and fully resistant equilibria. We approximate the basin of attraction for these cases. Moreover, all our calculations are reported with a precision of 3 significant digits.

3.3 Simulations of typical eco-evolutionary trajectories

Here we illustrate the behavior of trajectories inside and outside the basins of attraction of stable equilibria. We demonstrate how stable equilibria attract trajectories within their basins of attraction and how unstable equilibria repel trajectories outside these basins.

[1] If $u_R(0)$ exceeds 8 for the parameters in Table 2, $u_R(t)$ will grow unbounded.

Table 2 Parameters utilized in our simulations and approximation of basins of attraction

Parameter	g	K	α_{SS}	α_{RR}	k	b	m	σ	$r_{\max}$	α_{SR}	α_{RS}	d
Value	0.8	10^4	1	1	2	10	0.5	1	0.45 (cases 2,3) 0.35 (case 1)	0.15 (case 2) 1.15 (cases 1,3)	0.2 (case 2) 2 (cases 1,3)	0.01 (cases 2,3) 0.2 (case 1)

We simulate trajectories governed by (4), starting from various random initial conditions $(x_S(0), x_R(0), u_R(0))$. The parameter values used in these simulations are detailed in Table 2. For simulations, we consider three different cases mentioned before. In addition, all our calculations are reported with a precision of 3 significant digits.

4 Results

With substitutions

$$c_R(u_R, m) = r_{\max} e^{-g u_R} - d - \frac{m}{k + b u_R}, \quad c_{RR}(u_R) = \frac{r_{\max}}{K} e^{-g u_R},$$
$$c_S(m) = r_{\max} - d - \frac{m}{k}, \quad c_{SS} = \frac{r_{\max}}{K} \tag{5}$$

Equations (4) can be rewritten as

$$\begin{aligned}
\dot{x}_R &= x_R \Big(c_R(u_R, m) - \alpha_{RR} c_{RR}(u_R) x_R - \alpha_{RS} c_{RR}(u_R) x_S \Big) \\
\dot{x}_S &= x_S \Big(c_S(m) - \alpha_{SS} c_{SS} x_S - \alpha_{SR} c_{SS} x_R \Big) \\
\dot{u}_R &= \sigma \Big(- g\, r_{\max} e^{-g u_R} (1 - \frac{\alpha_{RR} x_R + \alpha_{RS} x_S}{K}) + \frac{b\, m}{(k + b u_R)^2} \Big)
\end{aligned} \tag{6}$$

The Jacobian matrix $J(x_S, x_R, u_R)$ of (6) is

$$\begin{pmatrix}
c_S(m) - c_{SS}(2\alpha_{SS} x_S + \alpha_{SR} x_R) & -\alpha_{SR} x_S & 0 \\
-\alpha_{RS} c_{RR}(u_R) x_R & c_R(u_R, m) - c_{RR}(u_R)(2\alpha_{RR} x_R + \alpha_{RS} x_S) & x_R \frac{\partial G_R}{\partial u_R} \\
\sigma g c_{RR}(u_R) \alpha_{RS} & \sigma g c_{RR}(u_R) \alpha_{RR} & \sigma \frac{\partial^2 G_R}{\partial u_R^2}
\end{pmatrix} \tag{7}$$

where G_R denotes $G(v, \mathbf{u}, \mathbf{x}, m)\Big|_{v=u_R}$.

4.1 Eco-evolutionary equilibria and their stability

We have four different potential equilibria of eco-evolutionary dynamics (6): interior, trivial, fully sensitive, and fully resistant equilibria, which will be analyzed in Sects. 4.1.1, 4.1.2, 4.1.3, and 4.1.4, respectively.

4.1.1 Interior equilibrium

If an interior equilibrium $\mathbf{x}^* = (x_S^*, x_R^*, u_R^*)^\top$ of (6) exists, it satisfies

$$x_R^*(m) = \frac{1}{\mathrm{D}} \Big(- \alpha_{RS} \frac{c_S(m)}{c_{SS}} + \alpha_{SS} \frac{c_R(u_R^*(m), m)}{c_{RR}(u_R^*(m))} \Big) \tag{8}$$

$$x_S^*(m) = \frac{1}{\mathrm{D}} \Big(\alpha_{RR} \frac{c_S(m)}{c_{SS}} - \alpha_{SR} \frac{c_R(u_R^*(m), m)}{c_{RR}(u_R^*(m))} \Big) \tag{9}$$

$$u_R^*(m) = \frac{-k}{b} + \frac{-mg + \sqrt{m^2 g^2 + 4mgdb}}{2bdg} \tag{10}$$

where

$$\mathrm{D} = \alpha_{SS}\alpha_{RR} - \alpha_{SR}\alpha_{RS}$$

Existence of the interior equilibrium (8–10) requires the following conditions:

1. Condition $k^2dg + kmg < mb$, which ensures that $u_R^*(m)$ is positive.
2. Equations (8) and (9) are positive.

Let us analyze when the second condition is satisfied. We will do so by considering two separate assumptions: $D < 0$ and $D > 0$, as $D = 0$ implies no interior equilibrium:

- Case $D > 0$. If $c_S(m) < 0$, $c_R(u_R^*(m), m)$ must be negative, otherwise $x_S^*(m)$ becomes negative. For (8) and (9) to become positive, the following has to be held:

$$\alpha_{SS}\frac{c_R(u_R^*(m),m)}{c_{RR}(u_R^*(m))} > \alpha_{RS}\frac{c_S(m)}{c_{SS}} \implies \frac{\alpha_{RS}}{\alpha_{SS}} > \frac{c_R(u_R^*(m),m)}{c_S(m)}e^{gu_R^*}$$
$$\alpha_{RR}\frac{c_S(m)}{c_{SS}} > \alpha_{SR}\frac{c_R(u_R^*(m),m)}{c_{RR}(u_R^*(m))} \implies \frac{\alpha_{RR}}{\alpha_{SR}} < \frac{c_R(u_R^*(m),m)}{c_S(m)}e^{gu_R^*}$$

  This implies $\frac{\alpha_{RR}}{\alpha_{SR}} < \frac{\alpha_{RS}}{\alpha_{SS}}$, and $D < 0$, a contradiction to our assumption that $D > 0$. Therefore, if $D > 0$, $c_S(m)$ must be positive to have an interior eco-evolutionary equilibrium of (4).
- Case $D < 0$. If $c_S(m) < 0$, $c_R(u_R^*(m), m)$ has to be negative, otherwise $x_R^*(m)$ becomes negative. For (8) and (9) to become positive the following has to be held:

$$\alpha_{SS}\frac{c_R(u_R^*(m),m)}{c_{RR}(u_R^*(m))} < \alpha_{RS}\frac{c_S(m)}{c_{SS}} \implies \frac{\alpha_{RS}}{\alpha_{SS}} < \frac{c_R(u_R^*(m),m)}{c_S(m)}e^{gu_R^*}$$
$$\alpha_{RR}\frac{c_S(m)}{c_{SS}} < \alpha_{SR}\frac{c_R(u_R^*(m),m)}{c_{RR}(u_R^*(m))} \implies \frac{\alpha_{RR}}{\alpha_{SR}} > \frac{c_R(u_R^*(m),m)}{c_S(m)}e^{gu_R^*}$$

  This implies $\frac{\alpha_{RR}}{\alpha_{SR}} > \frac{\alpha_{RS}}{\alpha_{SS}}$ and $D > 0$, a contradiction to our assumption that $D < 0$. Therefore, if $D < 0$, $c_S(m)$ has to be positive to have an interior eco-evolutionary equilibrium of (4).

We can conclude that regardless of the sign of D, the condition $c_S(m) > 0$ has to be satisfied for the existence of an interior equilibrium of (4).

Let us investigate local stability properties of the interior equilibrium (8–10). Eigenvalues of Jacobian (7) evaluated at the interior equilibrium (8–10) are:

$$\lambda_{1,2} = \frac{-(c_{RR}(u_R^*(m))\alpha_{RR}x_R^*(m) + c_{SS}\alpha_{SS}x_S^*(m))}{2} \pm \frac{S(m)}{2} \tag{11}$$

$$\lambda_3 = \sigma\frac{\partial^2 G}{\partial u_R^2}\bigg|_{u_R = u_R^*(m)} \tag{12}$$

where $S(m)$ is defined as

$$\sqrt{(c_{RR}(u_R^*(m))\alpha_{RR}x_R^*(m) + c_{SS}\alpha_{SS}x_S^*(m))^2 - 4c_{SS}c_{RR}(u_R^*(m))x_S^*(m)x_R^*(m)\cdot \mathrm{D}} \tag{13}$$

The eigenvalues (11) and (12) are calculated through expressing $c_S(m)$ and $c_R(u_R^*(m), m)$ through equations (8) and (9), as follows:

$$c_S(m) = c_{SS}\alpha_{SS}x_S^*(m) + c_{SS}\alpha_{SR}x_R^*(m) \tag{14}$$

$$c_R(u_R^*(m), m) = c_{RR}(u_R^*(m))\alpha_{RS}x_S^*(m) + c_{RR}(u_R^*(m))\alpha_{RR}x_R^*(m) \tag{15}$$

Through comparing equations $\dot{u}_R = 0$ and $\dot{x}_R = 0$, we can rewrite (12) into

$$\lambda_3 = \sigma \left(\frac{gbm}{(k + bu_R^*(m))^2} - \frac{2b^2 m}{(k + bu_R^*(m))^3} \right) = \frac{\sigma bm \left(g(k + bu_R^*(m)) - 2b \right)}{(k + bu_R^*(m))^3} \tag{16}$$

Theorem 1 *If the interior equilibrium* $\mathbf{x}^*$ *exists, it is locally stable if* $D = \alpha_{SS}\alpha_{RR} - \alpha_{SR}\alpha_{RS} > 0$.

Proof According to (11), if D $<$ 0, $S(m)$ defined by (13) becomes larger than $c_{RR}(u_R^*(m))\alpha_{RR}x_R^*(m) + c_{SS}\alpha_{SS}x_S^*(m)$. As a consequence, one of the eigenvalues (11) becomes positive. But if D $>$ 0, $S(m)$ from (13) becomes less than the term $c_{RR}(u_R^*(m))\alpha_{RR}x_R^*(m) + c_{SS}\alpha_{SS}x_S^*(m)$ and, subsequently, both eigenvalues (11) become negative.

Moreover, from (16), we can imply that if $k + bu_R^*(m) < \frac{2b}{g}$, the third eigenvalue λ_3 is also negative.

We can see that this is true from (10), which implies

$$-k - bu_R^*(m) = \frac{gm - \sqrt{g^2m^2 + 4gdbm}}{2dg} \tag{17}$$

Adding $\frac{2b}{g}$ to the both sides of (17) yields

$$\frac{2b}{g} - (k + bu_R^*(m)) = \frac{4bd + gm - \sqrt{g^2m^2 + 4gbdm}}{2dg} \tag{18}$$

By comparing $4bd + gm$ and $\sqrt{g^2m^2 + 4\,gbdm}$, we can see that (18) is positive and, indeed, $k + bu_R^*(m) < \frac{2b}{g}$ and λ_3 is always negative. Consequently, if the interior equilibrium (8–10) exists and corresponding D is positive, this equilibrium is locally stable. □

4.1.2 Trivial equilibrium

By a trivial equilibrium we mean an equilibrium with $x_S = x_R = 0$, while $\dot{u}_R = 0$, i.e.,

$$-gr_{\max}e^{-gu_R} + \frac{bm}{(k + bu_R)^2} = 0 \tag{19}$$

Let us refer to u_R solving (19) as $u_R^\diamond$ and to the trivial equilibrium as to $\mathbf{x}^\diamond$, where $\mathbf{x}^\diamond = (0, 0, u_R^\diamond)^\top$.

Note that (19) consists of a sum of an exponential function $gr_{\max}e^{-gu_R}$ and a reciprocal squared function $\frac{bm}{(k+bu_R)^2}$. Therefore, depending on the values of parameters g, $r_{\max}$, b, m, and k, this equation can have zero, one, or two solutions: If the value of the exponential function at $u_R = 0$ is greater than or equal to the value of the reciprocal squared function at $u_R = 0$, equation (19) will have one solution. Otherwise, equation (19) can have up to two solutions, which means we may have more trivial equilibria.

Eigenvalues of the Jacobian (7) evaluated at $x^\diamond$ are:

$$\lambda_1 = c_S(m) \tag{20}$$

$$\lambda_2 = c_R(u_R^\diamond, m) \tag{21}$$

$$\lambda_3 = \sigma \frac{\partial^2 G}{\partial u_R^2}\bigg|_{u_R = u_R^\diamond} \tag{22}$$

Using (19), we can rewrite (22) as follows:

$$\lambda_3 = \sigma\left(\frac{gbm}{(k+bu_R^\diamond)^2} - \frac{2b^2m}{(k+bu_R^\diamond)^3}\right) = \frac{\sigma bm}{(k+bu_R^\diamond)^2}\left(g - \frac{2b}{k+bu_R^\diamond}\right) \tag{23}$$

Theorem 2 *If a trivial equilibrium* $\mathbf{x}^\diamond$ *exists and additionally,* $c_S(m) < 0$, $c_R(u_R^\diamond, m) < 0$, *and* $k + bu_R^\diamond < \frac{2b}{g}$, *then* $\mathbf{x}^\diamond$ *is locally stable.*

Proof The trivial equilibrium $\mathbf{x}^\diamond$ is locally stable if the eigenvalues (20–22) have negative real parts, implying also that $c_S(m) < 0$ and $c_R(u_R^\diamond, m) < 0$. Equation (23) implies that $\frac{\sigma bm}{(k+bu_R^\diamond)^2}\left(g - \frac{2b}{k+bu_R^\diamond}\right) < 0$. This is equivalent to $k + bu_R^\diamond < \frac{2b}{g}$. Thus, if $c_S(m) < 0$, $c_R(u_R^\diamond, m) < 0$, and $k + bu_R^\diamond < \frac{2b}{g}$, while equation (19) has at least one solution, the trivial equilibrium will be locally stable. In this case, if the initial state is within the basin of attraction of $\mathbf{x}^\diamond$, then the corresponding trajectory will converge to $\mathbf{x}^\diamond$. □

4.1.3 Fully sensitive equilibrium

At this equilibrium, $x_R = 0$. Let us refer to this equilibrium as $\mathbf{x}^\dagger = (0, x_S^\dagger, u_R^\dagger)^\top$. Substitution of $x_R = 0$ in $\dot{x}_S = 0$ and $\dot{u}_R = 0$ yields the following expressions for $x_S^\dagger$ and $u_R^\dagger$:

$$x_S^\dagger = \frac{K}{\alpha_{SS}}\left(1 - \frac{1}{r_{\max}}\left(d + \frac{m}{k}\right)\right) \tag{24}$$

$$u_R^\dagger \in \left\{u_R \in \mathbb{R}^+ | -gr_{\max}e^{-gu_R}\left(1 - \frac{\alpha_{RS}x_S^\dagger}{K}\right) + \frac{bm}{(k+bu_R)^2} = 0\right\} \tag{25}$$

A similar argument as in case of (19) holds for (25), implying that (25) can have up to two solutions.

As $x_S^\dagger > 0$, it implies

$$d + \frac{m}{k} < r_{\max}$$

In addition, (25) implies:

$$gr_{\max}e^{-gu_R^\dagger}\left(1 - \frac{\alpha_{RS}x_S^\dagger}{K}\right) = \frac{bm}{(k+bu_R^\dagger)^2}$$

which leads to

$$1 - \frac{\alpha_{RS}x_S^\dagger}{K} > 0 \tag{26}$$

By substituting $x_S^\dagger$ from (24) to (26), we obtain:

$$c_S(m) < \frac{\alpha_{SS}}{\alpha_{RS}}r_{\max}$$

Thus, the existence of the fully sensitive equilibrium requires inequality

$$0 < c_S(m) < \frac{\alpha_{SS}}{\alpha_{RS}}r_{\max} \tag{27}$$

to be held.

Eigenvalues of the Jacobian (7) evaluated at $\mathbf{x}^\dagger$ are:

$$\lambda_1 = c_S(m) - 2c_{SS}\alpha_{SS}x_S^\dagger = -c_S(m) \tag{28}$$

$$\lambda_2 = c_R(u_R^\dagger, m) - c_{RR}(u_R^\dagger)\alpha_{RS}x_S^\dagger \tag{29}$$

$$\lambda_3 = \sigma \frac{\partial^2 G}{\partial u_R^2}\bigg|_{u_R = u_R^\dagger} \tag{30}$$

Using equations $\dot{u}_R = 0$ and $\dot{x}_R = 0$, we can rewrite (30) in the following way:

$$\lambda_3 = \sigma\left(\frac{gbm}{(k+bu_R^\dagger)^2} - \frac{2b^2m}{(k+bu_R^\dagger)^3}\right) = \frac{\sigma bm}{(k+bu_R^\dagger)^3}\left(g(k+bu_R^\dagger) - 2b\right) \tag{31}$$

Now we introduce $\kappa(u_R, m) = \alpha_{SS}\frac{c_R(u_R,m)}{c_{RR}(u_R)} - \alpha_{RS}\frac{c_S(m)}{c_{SS}}$. We can see from (8), that $x_R^*(m) = \frac{1}{\mathrm{D}}\kappa(u_R^*, m)$.

Theorem 3 *If $\mathbf{x}^\dagger$ exists, and additionally $c_S(m) > 0$, $\kappa(u_R^\dagger, m) < 0$, and $k + bu_R^\dagger < \frac{2b}{g}$, then $\mathbf{x}^\dagger$ is locally stable.*

Proof According to (28), if $c_S(m) > 0$, then $\lambda_1 < 0$.

By substituting (24) in (29), we can rewrite λ_2 in the following way:

$$\begin{aligned}\lambda_2 &= c_R(u_R^\dagger, m) - c_{RR}(u_R^\dagger)\alpha_{RS}x_S^\dagger \\ &= c_R(u_R^\dagger, m) - \frac{\alpha_{RS}}{\alpha_{SS}}c_{RR}(u_R^\dagger)\frac{c_S(m)}{c_{SS}} \\ &= \frac{c_{RR}(u_R^\dagger)}{\alpha_{SS}}\left(\alpha_{SS}\frac{c_R(u_R^\dagger(m), m)}{c_{RR}(u_R^\dagger(m))} - \alpha_{RS}\frac{c_S(m)}{c_{SS}}\right)\end{aligned} \tag{32}$$

We can see that $\lambda_2 = \frac{c_{RR}(u_R^\dagger)}{\alpha_{SS}}\kappa(u_R^\dagger, m)$. Thus, if $\kappa(u_R^\dagger, m) < 0$, λ_2 is negative.

Equation (31) implies that if $k + bu_R^\dagger < \frac{2b}{g}$, λ_3 becomes negative. Thus, if the conditions mentioned in the Theorem are satisfied, the fully sensitive equilibrium will become locally stable.

4.1.4 Fully resistant equilibrium

At this equilibrium, which we will denote by $\mathbf{x}^\ddagger = (x_S^\ddagger, x_R^\ddagger, u_R^\ddagger)^\top$, $x_S^\ddagger = 0$, while $x_R = x_R^\ddagger$ and $u_R = u_R^\ddagger$, with

$$x_R^\ddagger = \frac{K}{\alpha_{RR}}\left(1 - \frac{1}{r_{\max}e^{-gu_R^\ddagger}}(d + \frac{m}{k+bu_R^\ddagger})\right) \tag{33}$$

$$u_R^\ddagger \in \left\{u_R \in \mathbb{R}^+ | -gr_{\max}e^{-gu_R}\left(1 - \frac{\alpha_{RR}x_R^\ddagger}{K}\right) + \frac{bm}{(k+bu_R)^2} = 0\right\} \tag{34}$$

Positivity of the right-hand side of (33) implies

$$r_{\max}e^{-gu_R^\ddagger} > d + \frac{m}{k+bu_R^\ddagger} \implies c_R(u_R^\ddagger, m) > 0 \tag{35}$$

In addition, α_{RR} does not have any effects on the positivity of $u_R^\ddagger$, since α_{RR} in (34) will be canceled out by itself in (33).

Substituting (33) to (34) yields:

$$-gd - \frac{gm}{k + bu_R^{\ddagger}} + \frac{bm}{(k + bu_R^{\ddagger})^2} = 0 \tag{36}$$

Now we introduce the next lemma, which is used for calculating $u_R^{\ddagger}$.

Lemma 1 *Consider the function*

$$\Xi(u_R, m) = -gd - \frac{gm}{k + bu_R} + \frac{bm}{(k + bu_R)^2} \tag{37}$$

where $\Xi(u_R, m) = 0$ *for* $u_R = u_R^*(m)$. *For* $u_R < u_R^*(m)$, *the function* $\Xi(u_R, m) > 0$, *while for* $u_R > u_R^*(m)$, $\Xi(u_R, m) < 0$.

Proof By rewriting dynamics of u_R as

$$\dot{u}_R = \sigma\Bigg(- g\frac{\dot{x}_R}{x_R} \underbrace{-gd - \frac{gm}{k + bu_R} + \frac{bm}{(k + bu_R)^2}}_{\Xi(u_R, m)} \Bigg) \tag{38}$$

at $u_R^*(m)$ we have:

$$-gd - \frac{gm}{k + bu_R^*(m)} + \frac{bm}{(k + bu_R^*(m))^2} = 0 \tag{39}$$

Thus, at $u_R^*(m)$,

$$-gd(k + bu_R^*(m))^2 - gm(k + bu_R^*(m)) + bm = 0 \tag{40}$$

Multiplying $\Xi(u_R, m)$ by u_R yields:

$$\Xi(u_R, m)(k + bu_R)^2 = -gd(k + bu_R)^2 - gm(k + bu_R) + bm \tag{41}$$

Now we can subtract (40) from (41):

$$\begin{aligned}\Xi(u_R, m)(k + bu_R)^2 - 0 = &-gd(k + bu_R)^2 - gm(k + bu_R) + bm \\ &- (-gd(k + bu_R^*(m))^2 - gm(k + bu_R^*(m)) + bm)\end{aligned}$$

After some algebraic manipulations, we obtain:

$$\Xi(u_R, m)(k + bu_R)^2 = -gb(u_R - u_R^*(m))\Big(d(2k + bu_R + bu_R^*) + m\Big) \tag{42}$$

By comparing both sides of (42), we can see the sign of $\Xi(u_R, m)(k + bu_R)^2$ is opposite to the sign of $u_R - u_R^*(m)$. Consequently, for $u_R > u_R^*(m)$, we get $\Xi(u_R, m) < 0$, and for $u_R < u_R^*(m)$, we get $\Xi(u_R, m) > 0$. □

According to Lemma 1, and by comparing (36) with (40), we can see that $u_R^{\ddagger} = u_R^*(m)$. Eigenvalues of the Jacobian (7) evaluated at $\mathbf{x}^{\ddagger}$ are:

$$\lambda_1 = c_S(m) - c_{SS}\alpha_{SR}x_R^{\ddagger} \tag{43}$$

$$\lambda_2 = c_R(u_R^{\ddagger}, m) - 2c_{RR}(u_R^{\ddagger})\alpha_{RR}x_R^{\ddagger} = -c_R(u_R^{\ddagger}, m) \tag{44}$$

$$\lambda_3 = \sigma\frac{\partial^2 G}{\partial u_R^2}\bigg|_{u_R = u_R^{\ddagger}} \tag{45}$$

Using (34), we can rewrite (45) as follows:

$$\lambda_3 = \sigma\left(\frac{gbm}{(k+bu_R^{\ddagger})^2} - \frac{2b^2m}{(k+bu_R^{\ddagger})^3}\right) = \frac{\sigma bm}{(k+bu_R^{\ddagger})^3}\left(g(k+bu_R^{\ddagger}) - 2b\right) \tag{46}$$

Theorem 4 *If* $\mathbf{x}^{\ddagger}$ *exists, and additionally* $c_R(u_R^{\ddagger}, m) > 0$ *and* $D \cdot x_S^* < 0$, *then* $\mathbf{x}^{\ddagger}$ *is locally stable.*

Proof Equation (43) can be rewritten as

$$\begin{aligned}
\lambda_1 &= c_S(m) - c_{SS}\alpha_{SR}x_R^{\ddagger} \\
&= c_{SS}\left(\frac{c_S(m)}{c_{SS}} - \frac{\alpha_{SR}}{\alpha_{RR}}K\left(1 - \frac{1}{r_{\max}e^{-gu_R^*(m)}}\left(d + \frac{m}{k+bu_R^*(m)}\right)\right)\right) \\
&= c_{SS}\left(\frac{c_S(m)}{c_{SS}} - \frac{\alpha_{SR}}{\alpha_{RR}}\frac{K}{r_{\max}e^{-gu_R^*(m)}}c_R(u_R^*(m), m)\right) \\
&= c_{SS}\left(\frac{c_S(m)}{c_{SS}} - \frac{\alpha_{SR}}{\alpha_{RR}}\frac{c_R(u_R^*(m), m)}{c_{RR}(u_R^*(m))}\right)
\end{aligned} \tag{47}$$

Comparing (47) with (9), we obtain

$$\lambda_1 = c_{SS}\frac{\mathrm{D} \cdot x_S^*}{\alpha_{RR}} \tag{48}$$

Thus, if $\mathrm{D} \cdot x_S^* < 0$, then $\lambda_1 < 0$. Moreover, since $u_R^{\ddagger} = u_R^*(m)$, similarly to what we showed in subsection 4.1.1, we can conclude that $k + bu_R^{\ddagger} < \frac{2b}{g}$, and, as a result, λ_3 is always negative. Consequently, if $c_R(u_R^{\ddagger}, m)$ is positive and $\mathrm{D} \cdot x_S^*$ is negative, all corresponding eigenvalues are negative, and the fully resistant equilibrium is locally stable.

Note that when $D = 0$, (47) implies that instead of the sign of $\mathrm{D} \cdot x_S^*$, we should check the sign of $\frac{c_S(m)}{c_{SS}} - \frac{\alpha_{SR}}{\alpha_{RR}}\frac{c_R(u_R^*(m),m)}{c_{RR}(u_R^*(m))}$. And when we substitute c_{SS} and $c_{RR}(u_R^*(m))$ from into the previous term, that turns into $c_S(m)e^{-gu_R^*} - \frac{\alpha_{SR}}{\alpha_{RR}}c_R(u_R^*(m), m)$.

4.1.5 Effect of competition coefficients on different equilibria

Equation (8) and Theorem 1 imply that for x_R^* to be positive, it is required that $c_S(m) > 0$ and

$$\frac{\alpha_{RS}}{\alpha_{SS}} < \frac{c_R(u_R^*(m), m)}{c_S(m)}e^{gu_R^*} \tag{49}$$

Moreover, (27) implies:

$$\frac{\alpha_{RS}}{\alpha_{SS}} < \frac{r_{\max}}{c_S(m)}$$

Further, (5) leads to

$$\frac{c_R(u_R^*(m), m)}{c_S(m)}e^{gu_R^*} < \frac{r_{\max}}{c_S(m)}$$

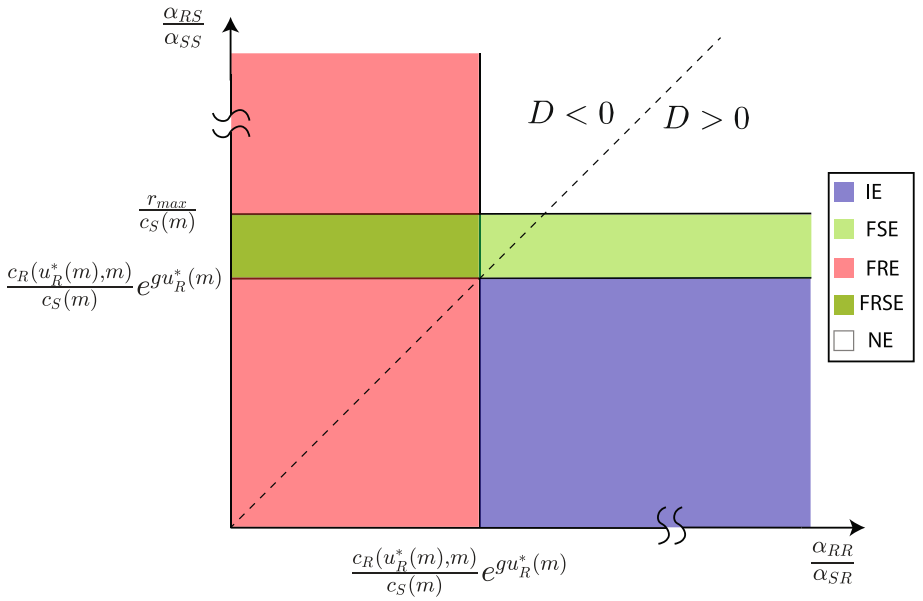

Fig. 1 Different types of equilibria in the $(\frac{\alpha_{RS}}{\alpha_{SS}}, \frac{\alpha_{RR}}{\alpha_{SR}})$-plane when $c_S(m)$ is positive. Abbreviations: IE - stable interior equilibrium, FSE - stable fully sensitive equilibrium, FRE - stable fully resistant equilibrium, FRSE - stable fully sensitive and fully resistant equilibria, NE - no stable equilibrium

Thus, when $c_S(m) > 0$, $\frac{\alpha_{RS}}{\alpha_{SS}}$ determines whether the cancer dynamics have stable fully sensitive equilibria (FSE) or not. If

$$\frac{c_R(u_R^*(m), m)}{c_S(m)} e^{gu_R^*} < \frac{\alpha_{RS}}{\alpha_{SS}} < \frac{r_{\max}}{c_S(m)}, \tag{50}$$

the dynamics (4) have at least one stable FSE. But, if

$$\frac{r_{\max}}{c_S(m)} < \frac{\alpha_{RS}}{\alpha_{SS}} \tag{51}$$

the dynamics (4) have no stable FSE. Moreover, (9), and Theorem 1 imply that for x_S^* to be positive, inequalities $c_S(m) > 0$ and

$$\frac{\alpha_{SR}}{\alpha_{RR}} < \frac{c_S(m)}{c_R(u_R^*(m), m)} e^{-gu_R^*} \tag{52}$$

have to be held. In addition, (47) implies that for the existence of a stable fully resistant equilibrium (FRE), the following has to be held:

$$\frac{\alpha_{SR}}{\alpha_{RR}} > \frac{c_S(m)}{c_R(u_R^*(m), m)} e^{-gu_R^*} \tag{53}$$

From (49–53), we can determine the type of locally stable equilibria in the $\left(\frac{\alpha_{RS}}{\alpha_{SS}}, \frac{\alpha_{RR}}{\alpha_{SR}}\right)$-plane when $c_S(m) > 0$, as demonstrated in Fig. 1.

If $c_S(m) < 0$, the signs of $c_R(u_R^{\diamond}, m)$ and $c_R(u_R^{\ddagger}, m)$ determine the existence of the stable trivial and fully resistant equilibria, respectively.

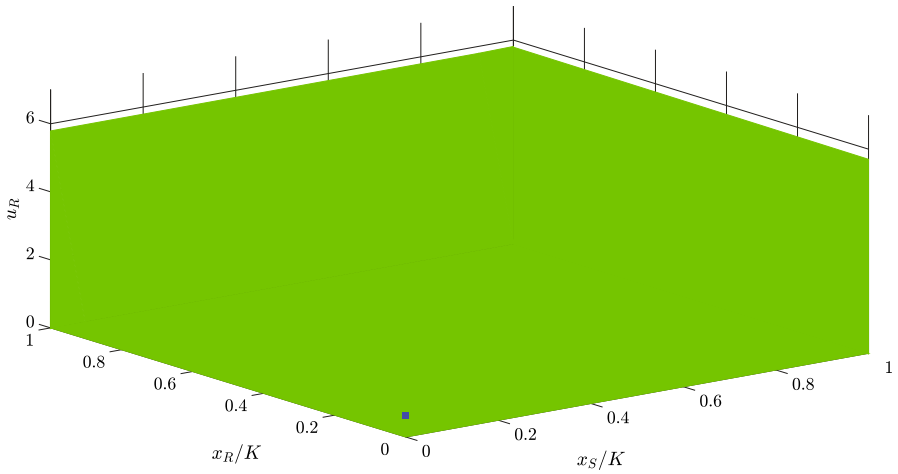

Fig. 2 Estimation of the basin of attraction (green) of the locally stable trivial equilibrium (blue). Parameter values: $r_{\max} = 0.350$, $g = 0.800$, $K = 10000$, $\alpha_{SS} = \alpha_{RR} = 1$, $\alpha_{SR} = 1.150$, $\alpha_{RS} = 2$, $d = 0.200$, $m = 0.500$, $k = 2$, $b = 10$, and $\sigma = 1$

Figure 1 shows that when the net growth rate $c_S(m)$ of sensitive cells is positive, the existence of an FRE is dependent on the ratio of competition coefficients α_{RR} and α_{SR}. If $\frac{\alpha_{RR}}{\alpha_{SR}}$ is less than $\Gamma = \frac{c_R(u_R^*(m),m)}{c_S(m)} e^{g u_R^*}$, the cancer dynamics will have an FRE. But if $\frac{\alpha_{RR}}{\alpha_{SR}}$ is greater than Γ, the cancer dynamics can have an IE if $\frac{\alpha_{RS}}{\alpha_{SS}}$ is less than Γ. The existence of an FSE depends on the ratio of competition coefficients α_{SS} and α_{RS}. If $\frac{\alpha_{RS}}{\alpha_{SS}}$ lies between $\frac{r_{\max}}{c_S(m)}$ and Γ, the cancer dynamics will have an FSE. Furthermore, if at the same time $\frac{\alpha_{RR}}{\alpha_{SR}} < \Gamma$, the cancer dynamics will have one FSE and one FRE.

4.2 Estimating basins of attraction

Case 1: In this case, we have one locally stable trivial equilibrium. Parameters for this case are mentioned in Table 2. One can obtain:

$$x_S^* = 1440.000, \quad x_R^* = -2871.000, \quad u_R^* = 0.248, \quad u_R^\diamond \in \{0.271, 7.135\}$$
$$\mathrm{D} = -1.300, \quad c_S(m) = -0.100, \quad c_R(u_R^\diamond, m)\Big|_{u_R^\diamond = 0.271} = -0.024$$

Since $k + b u_R^\diamond > \frac{2b}{g}$ for $u_R^\diamond = 7.135$, trivial equilibrium $(0, 0, 7.135)^\top$ is unstable. Thus, there exists only one locally stable trivial equilibrium: $(0, 0, 0.271)^\top$ The obtained estimation of the basin of attraction of the locally stable trivial equilibrium is shown in Fig. 2.

Case 2: In this case, we approximate the basin of attraction for one locally stable interior equilibrium. Using parameters in Table 2, we obtain

$$x_S^* = 3197.000, \quad x_R^* = 6833.000, \quad u_R^* = 0.835$$

Since the three-dimensional basin of attraction is easier to see from the two-dimensional projections, we plot such projections on the $(x_S/K\,, x_R/K)$- and $(x_R/K\,, u_R)$-planes in Fig. 3. In these figures, the interior equilibrium is highlighted by a blue square.

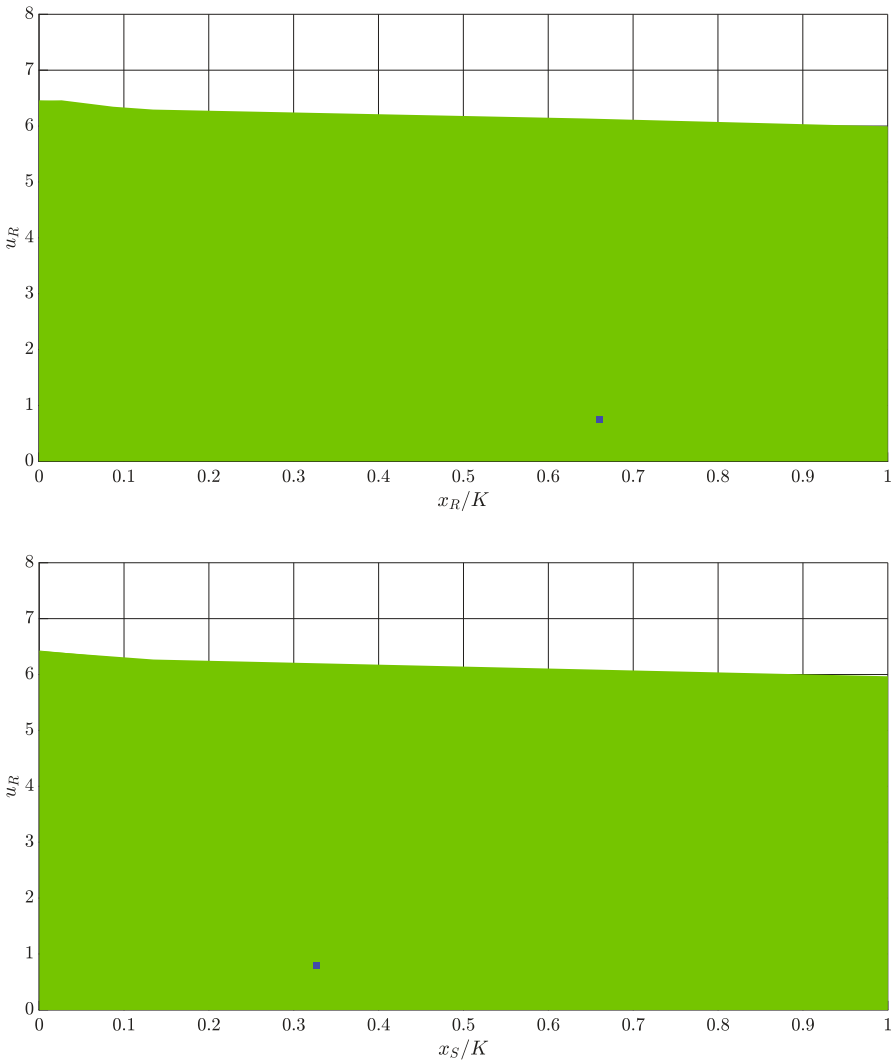

Fig. 3 Projections of the basin of attraction (green) of the locally stable interior equilibrium (blue) on the $(x_S/K, x_R/K)$-and $(x_R/K, u_R)$-planes. Parameter values: $r_{\max} = 0.450$, $g = 0.800$, $K = 10000$, $\alpha_{SS} = \alpha_{RR} = 1$, $\alpha_{SR} = 0.150$, $\alpha_{RS} = 0.200$, $d = 0.010$, $m = 0.500$, $k = 2$, $\sigma = 1$, and $b = 10$

From Figs. 2 and 3, we can see that the basins of attraction for both the trivial and interior equilibria are determined by u_R. This shows that the initial resistance rate is more important than the initial population size of cancer cells for delineating the basin of attraction of a stable equilibrium.

Case 3: In this case, dynamics (4) has one fully sensitive and one fully resistant locally stable equilibria. With values from Table 2, we obtain:

$$x_S^* = 3363.000, \quad x_R^* = 747.000, \quad u_R^* = u_R^{\ddagger} = 0.835$$
$$x_S^{\dagger} = 4222.000, \quad u_R^{\dagger} \in \{1.571, 3.205\}, \quad u_R^{\diamond} \in \{0.204, 7.604\}$$

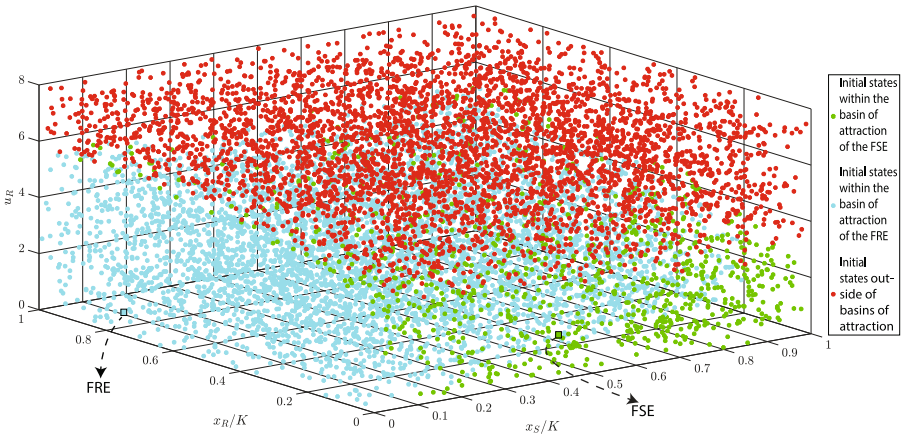

Fig. 4 Estimation of basins of attractions of two locally stable equilibria of (1–2). Parameter values: $r_{\max} = 0.450$, $g = 0.800$, $K = 10000$, $\alpha_{SS} = \alpha_{RR} = 1$, $\alpha_{SR} = 1.150$, $\alpha_{RS} = 2$, $d = 0.010$, $m = 0.500$, $k = 2$, $b = 10$, and $\sigma = 1$. Abbreviations: FRE - fully resistant equilibrium, FSE - fully sensitive equilibrium

$$x_R^{\ddagger} = 7472.000, \quad \mathrm{D} = -1.300, \quad c_S(m) = 0.190$$

Among the two possible values of $u_R^{\dagger}$, only $u_R^{\dagger} = 1.571$ satisfies $k + bu_R^{\dagger} < \frac{2b}{g}$. Thus, $(x_S^{\dagger}, 0, 3.205)^{\top}$ is unstable, while $(x_S^{\dagger}, 0, 1.571)^{\top}$ is locally stable. Moreover, as $c_R(u_R^{\ddagger}, m)$ is positive and $\mathrm{D}.x_S^* < 0$ is negative, $(0, x_R^{\ddagger}, u_R^{\ddagger})^{\top}$ is locally stable. In the following simulation, we normalize populations x_i of cancer cells $i \in \{R, S\}$ to x_i/K.

In Fig. 4, we estimate basins of attractions of the two locally stable equilibria. The fully resistant and fully sensitive equilibria are highlighted by blue and green squares, respectively. Moreover, the basins of attraction of the fully resistant and fully sensitive equilibria are estimated through blue and green dots. Starting from initial conditions highlighted by red dots results in an uncontrollable growth of u_R. Projections of the basins of attraction on the two-dimensional planes are shown in Fig. 5.

From Fig. 5, we can see that when cancer dynamics have two stable equilibria, the basin of attraction is determined mainly by u_R and x_R. This shows that the initial resistance rate and the initial population size of resistant cells are more important than the initial population size of sensitive cells for distinguishing the basins of attraction of an FRE and an FSE.

4.3 Simulations of typical cancer trajectories

Case 1: In this case, we will see the trajectories that are absorbed by the locally stable trivial equilibrium and those that are repelled from the unstable trivial equilibrium. We saw that we have one locally stable and one locally unstable trivial equilibrium in this case.

In Fig. 6, we execute the simulation for 80 different initial conditions. In this figure, the locally stable trivial equilibrium is shown with a blue circle, while the unstable equilibrium is demonstrated with a red square. The initial conditions that end up in the stable equilibrium are illustrated by green circles, while the ones that result in an uncontrollable growth of resistance rate are highlighted by red circles. Moreover, the projections of these trajectories on the $(x_S/K, u_R)$-plane and $(x_R/K, u_R)$-plane are illustrated in Fig. 6.

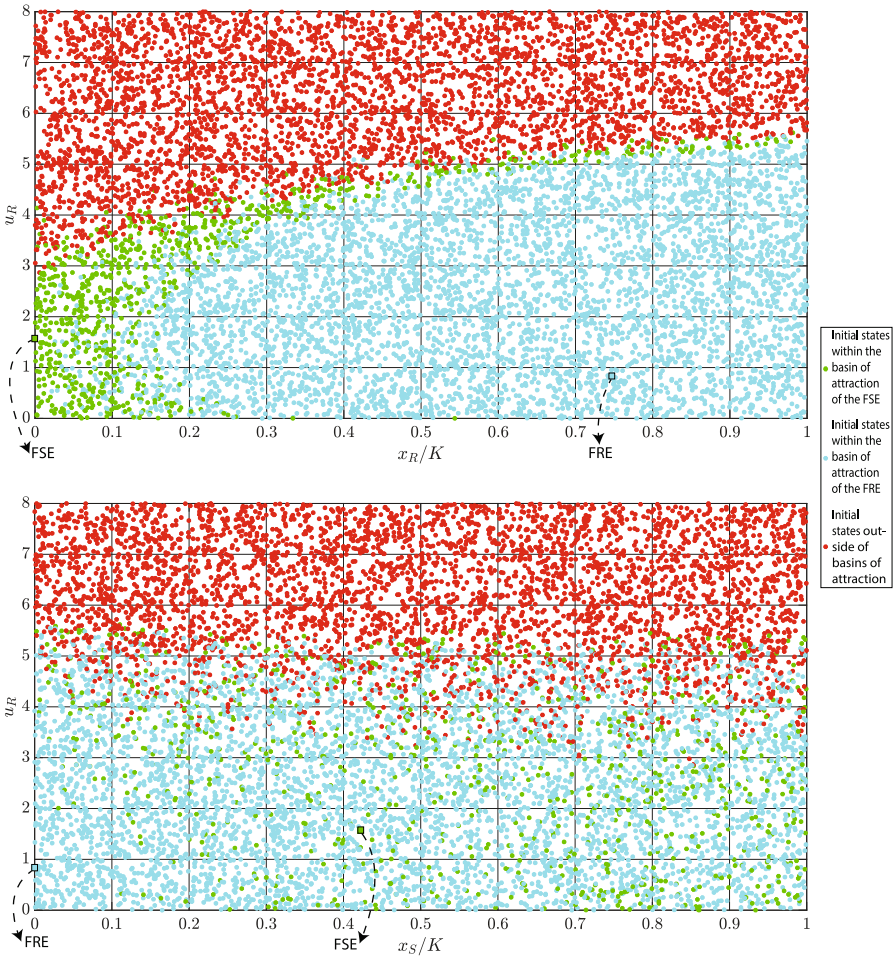

Fig. 5 Projections of basins of attraction on the $(x_S/K, u_R)$ and $(x_R/K, u_R)$ planes. Parameter values: $r_{\max} = 0.450$, $g = 0.800$, $K = 10000$, $\alpha_{SS} = \alpha_{RR} = 1$, $\alpha_{SR} = 1.150$, $\alpha_{RS} = 2$, $d = 0.010$, $m = 0.500$, $k = 2$, $b = 10$, and $\sigma = 1$. Abbreviations: FRE - fully resistant equilibrium, FSE - fully sensitive equilibrium

Case 2: As mentioned in Sect. 4.2, in this case, we have one locally stable interior equilibrium. Using parameters in Table 2, we can calculate the following:

$$\frac{x_S^\dagger}{K} = 0.422, \quad \frac{x_R^\ddagger}{K} = 0.747, \quad u_R^* = u_R^\ddagger = 0.835$$
$$u_R^\diamond \in \{0.204, 7.604\}, \quad u_R^\dagger \in \{0.226, 7.441\}, \quad \mathrm{D} = 0.970$$

In this case, $\mathrm{D} \cdot x_S^* > 0$ and, as a result, the fully resistant equilibrium is unstable. Also, both trivial equilibria are unstable since $c_S(m) > 0$. Dynamics (4) has two fully sensitive equilibria in this case. Since $\kappa(0.226, m) = 0.259 > 0$, the equilibrium $(x_S^\dagger, 0, 0.226)^\top$ is unstable. Moreover, for $u_R^\dagger = 7.441$ we have $k + bu_R^\dagger < \frac{2b}{g} = 25$, and, consequently, this trivial equilibrium is unstable, too. Figure 7 demonstrates projections of trajectories starting from 60 different initial conditions on the $(x_S, K - u_R)$- and $(x_R, K - u_R)$-planes.

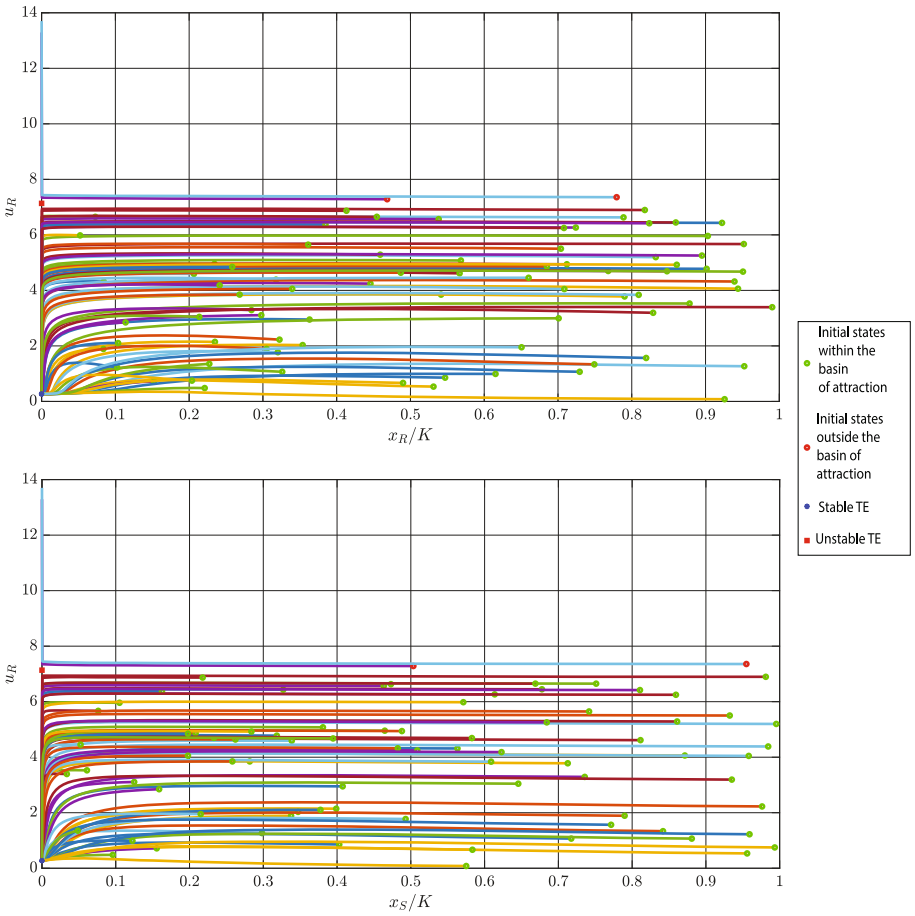

Fig. 6 Projections of various eco-evolutionary trajectories starting from different initial conditions on the $(x_S/K, u_R)$-plane and $(x_R/K, u_R)$-plane. In this case, we have two trivial equilibria (TE): The blue star denotes the locally stable equilibrium, while the red square denotes the unstable trivial equilibrium. Parameter values: $r_{\max} = 0.35$, $g = 0.8$, $K = 10000$, $\alpha_{SS} = \alpha_{RR} = 1$, $\alpha_{SR} = 1.15$, $\alpha_{RS} = 2$, $d = 0.2$, $m = 0.5$, $k = 2$, $b = 10$, and $\sigma = 1$

From Figs. 6 and 7, we can see that the resistance rate of the unstable trivial equilibrium delineates the border of the basin of attraction of the stable equilibrium.

Case 3: In this case, dynamics (4) have one fully sensitive and one fully resistant locally stable equilibria. Using parameter values from Table 2, we obtain:

$$x_S^* = 3363.000, \quad x_R^* = 747.000, \quad u_R^* = u_R^{\ddagger} = 0.835$$
$$x_S^{\dagger} = 4222.000, \quad u_R^{\dagger} \in \{1.571, 3.205\}, \quad u_R^{\diamond} \in \{0.204, 7.604\}$$
$$x_R^{\ddagger} = 7472.000, \quad \mathrm{D} = -1.300, \quad c_S(m) = 0.190$$

In this example, the interior equilibrium exists, but it is unstable, since $\mathrm{D} < 0$. Also, $c_S(m) > 0$, and, as a result, the trivial equilibrium is unstable as well. For $u_R^{\dagger} = 1.571$, $k + bu_R^{\dagger} < \frac{2b}{g}$ and for $u_R^{\dagger} = 3.205$, $k + bu_R^{\dagger} > \frac{2b}{g}$. Thus, $(x_S^{\dagger}, 0, 3.205)^{\top}$ is unstable, while $(x_S^{\dagger}, 0, 1.571)^{\top}$

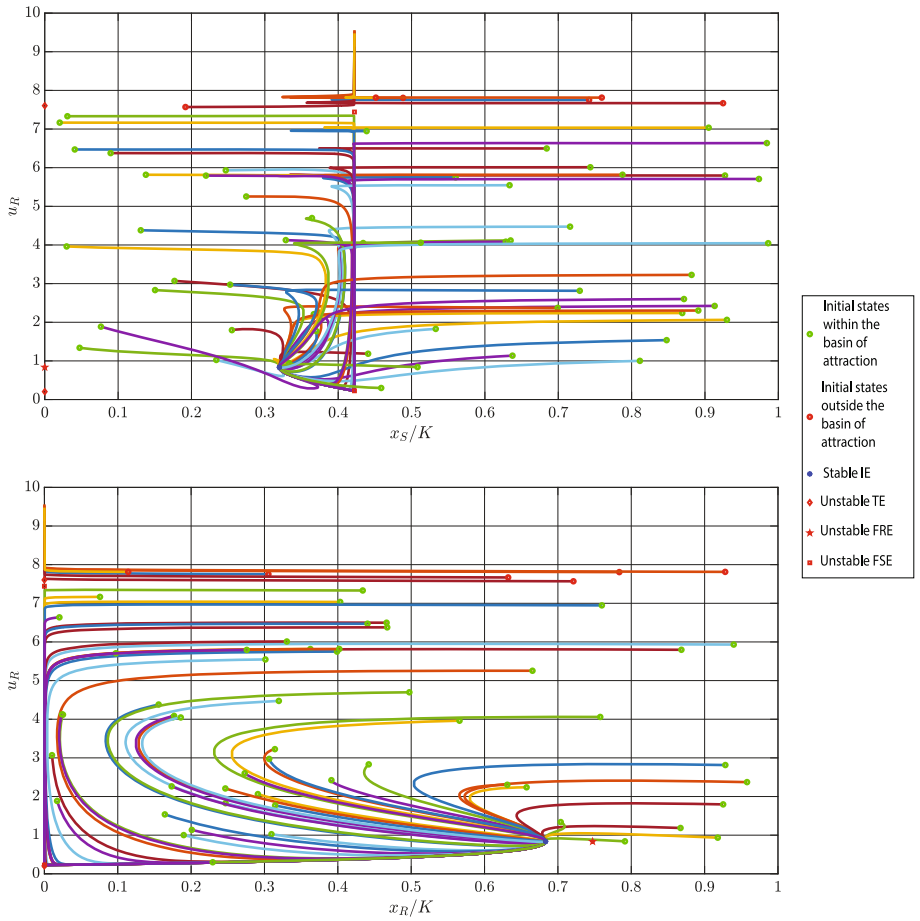

Fig. 7 Projection of trajectories starting from different initial conditions on the $(x_S/K, u_R)$- and $(x_R/K, u_R)$-planes. In this case, we have one locally stable interior equilibrium (IE). The blue star denotes the locally stable equilibrium, while the red square, red pentagon, and red diamond denote the unstable fully sensitive (FSE), fully resistant (FRE), and trivial equilibria (TE), respectively. Parameter values: $r_{\max} = 0.45$, $g = 0.8$, $K = 10000$, $\alpha_{SS} = \alpha_{RR} = 1$, $\alpha_{SR} = 0.15$, $\alpha_{RS} = 0.2$, $d = 0.01$, $m = 0.5$, $k = 2$, $b = 10$, and $\sigma = 1$

is locally stable. Moreover, $c_R(u_R^{\ddagger}, m) > 0$, $\mathrm{D}.x_S^* < 0$ and, consequently, $(0, x_R^{\ddagger}, u_R^{\ddagger})^{\top}$ is locally stable.

In Fig. 8, we demonstrate trajectories started from different initial conditions. One can see the trajectories that are absorbed by both locally stable FSE and locally stable FRE, and those that are repelled by unstable equilibria.

Since we projected three-dimensional trajectories onto two-dimensional planes, some trajectories appear to exhibit sudden changes. However, in the full three-dimensional space, no such sudden changes exist.

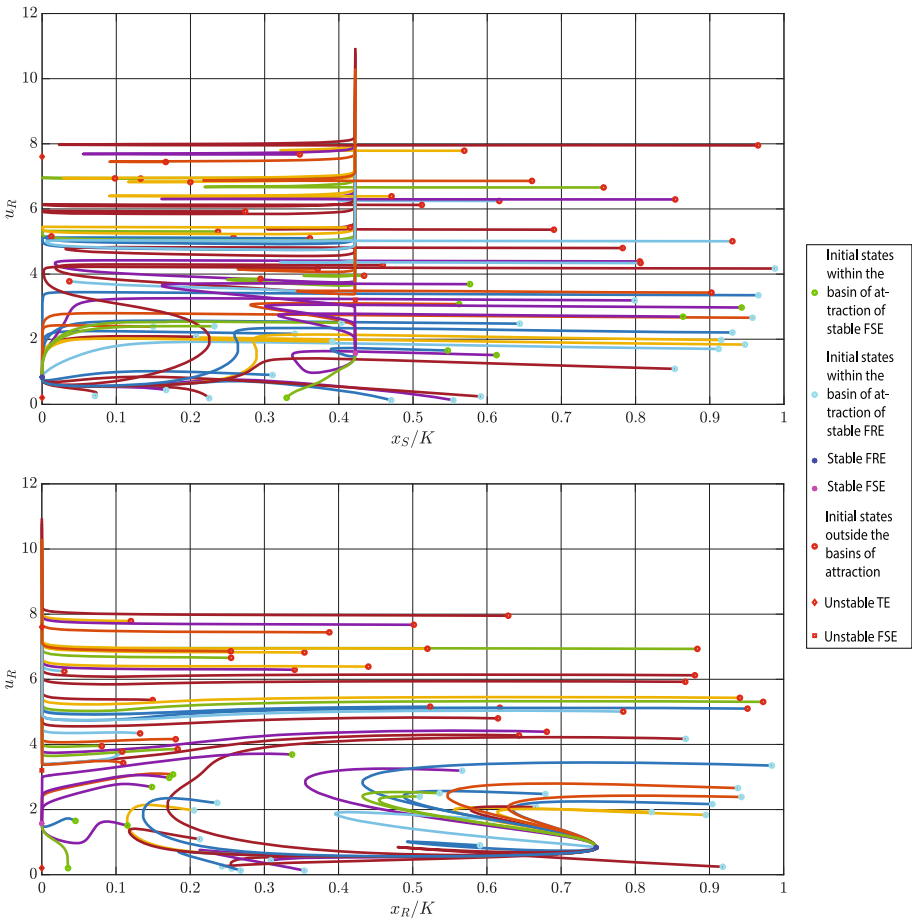

Fig. 8 Projection of trajectories starting from different initial conditions on both $(x_S/K, u_R)$- and $(x_R/K, u_R)$-planes. In this case, we have one locally stable fully resistant equilibrium (FRE) and one locally stable fully sensitive equilibrium (FSE). This figure estimates which states are in the basins of attraction of these two locally stable equilibria. Parameter values: $r_{\max} = 0.450$, $g = 0.800$, $K = 10000$, $\alpha_{SS} = \alpha_{RR} = 1$, $\alpha_{SR} = 1.150$, $\alpha_{RS} = 2$, $d = 0.010$, $m = 0.500$, $k = 2$, $b = 10$, and $\sigma = 1$

5 Discussion

In this paper, we analyzed a polymorphic Darwinian dynamics model under human intervention and studied its stability with respect to intraspecific competition and intensity of human intervention. As a specific example of such a Darwinian system, we took cancer under treatment. We analyzed how this system's eco-evolutionary equilibria depend on competition coefficients and treatment dose. We demonstrated that Darwinian dynamics lead to four different equilibria that can be stable or unstable, depending on the intensity of the human intervention and intraspecific competition. In the cancer treatment case study, we demonstrated that when the treatment dose is sufficiently low to maintain a positive net growth rate of sensitive cells, the system can reach three possible equilibria, depending on the intraspecific competition: (1) interior equilibrium when both effects of sensitive cells on resistant ones

and resistant cells on sensitive ones are not too high, (2) fully resistant equilibrium when the effect of resistant cells on sensitive ones is too high, (3) fully sensitive equilibrium when the effect of sensitive cells on resistant ones is neither too high nor too low. Moreover, we showed that when the treatment dose is higher than a threshold, which results in a negative net growth rate of sensitive cells, the system can reach either a fully resistant equilibrium or a trivial equilibrium (extinction of cancer cells) with higher treatment doses. We also approximated basins of attraction of different equilibria using the level-set method. We demonstrated typical eco-evolutionary trajectories of cancer cells within and outside these basins of attraction through simulations.

Our results strengthen our understanding of the stability of evolutionary games. While the stability of different types of dynamic games has been studied extensively [46–51] and also properties of evolutionarily stable equilibria, including their stability, are well defined and understood [34, 52–54], we believe our study is the first one that focuses specifically on the impact of both human intervention and competition coefficients on eco-evolutionary stability. Goh found conditions for globally asymptotically stable equilibria in Lotka-Volterra dynamics [55]. The most closely related work to ours is that of Mougi who added evolutionary dynamics to Lotka-Volterra two-species model with an allelopathic interaction and showed under what conditions these dynamics oscillate or stabilize on an equilibrium by depending on the evolutionary speed [56]. Here, we added evolutionary dynamics to competitive Lotka-Volterra ecological dynamics under human intervention and demonstrated that there are no globally stable equilibria.

Our results contribute to mathematical oncology as we consider cancer treatment as our main case study. Most existing literature in mathematical oncology uses models with qualitative type of resistance, thus explicitly not considering the evolution of resistance [57–65]. This literature often focuses on treatment protocols for containing tumor burden for as long time as possible. The limited mathematical oncology literature that utilizes models similar to the one introduced in this paper, i.e., models considering resistance as a quantitative evolving trait, mostly assumes either a monomorphic cancer population or a polymorphic population with no competition coefficients, which both lead to no interior eco-evolutionary equilibria [23, 31, 66–68]. Such models are often utilized for treatment optimization with respect to various measurable outcomes, such as time to progression or variance of tumor burden. Adding competition to the polymorphic Darwinian dynamics of cancer, one can focus on therapies stabilizing the eco-evolutionary dynamics of cancer at their interior equilibria, in the spirit of ongoing clinical trial in metastatic ovarian cancer (NCT05080556 [69]). Moreover, our model can be extended to allow for double-bind and extinction therapies, which are novel evolutionary therapies currently tested in initial clinical trials (NCT04343365) [70, 71].

Although we focused on cancer treatment as the main application of our work in this manuscript, the same results can be applied to similar case studies such as antibiotic resistance and pest management. For instance, according to our results in pest management, we should never use pesticides extensively unless there exists a stable trivial equilibrium for the dynamic of evolution of the pest population. If no stable trivial equilibrium exists, one should aim at stabilizing pest population at the interior or fully sensitive or resistant equilibria by using fewer pesticides.

How can physicians use our results? If a stable trivial equilibrium exists, a physician can do so by applying a sufficiently high dose of treatment corresponding to that stable trivial equilibrium and can eradicate all cancer cells. If no stable trivial equilibrium exists and sensitive cells do not evolve, a physician should check the existence of a stable fully sensitive equilibrium. If it exists and tumor volume at this equilibrium is tolerable for the patient, the physician should stabilize the tumor on this fully sensitive equilibrium. If no trivial and fully

sensitive equilibrium exists, the physician should aim at stabilizing the tumor on the interior or fully resistant equilibrium. This also depends on the tumor burden at these equilibria. If the corresponding tumor burden is not tolerable for the patient or no stable equilibria exist, the physician should consider maximizing time to progression with the current treatment or using multi-drug therapy [72–74].

To make the results of the case study on cancer treatment presented in this paper applicable in the real world, we need to fit our model to patient time-series data, such as volumetric data (e.g., through serum biomarkers or imaging) [75–77] or information on different cancer cell types (e.g., liquid biopsies [78–80]). While for some cancers, such as prostate cancer, such information is easy to find (prostate-specific antigen; [81]), for other cancers, such as non-small cell lung cancer, we rely on imaging and liquid biopsies. Measuring resistance rate may be (nearly) impossible and must be estimated through time-series data, thus availability of such data is a must.

While this paper focused on equilibria of eco-evolutionary dynamics, future research directions should aim at stabilizing the dynamics at desirable equilibria through optimal control, similarly as it was done in simpler models before in [64, 82–84].

Our model of Darwinian dynamics presented here has some limitations, especially as it approximates evolutionary dynamics less well when the distribution of evolutionary traits is multi-modal or, for example, in the case of disruptive selection [85, 86]. Lion et al. have proposed to apply moment closure approximation to solve this problem [87]. Future research should address how different distributions of evolutionary dynamics impact our ability to capture the eco-evolutionary system in question through Darwinian dynamics and/or how to approximate these dynamics more precisely.

Acknowledgements We thank our colleagues from the EvoGamesPlus project for the discussions and recommendations that eventually led to this paper. We especially thank Dr. Yannick Viossat and Dr. Mark Broom for their valuable feedback and discussions, which shaped the current form of the paper.

Author Contributions Mohammadreza Satouri: Conceptualization, Formal analysis, Methodology, Software, Visualization, Writing- Original draft preparation, Writing- Reviewing and Editing. Jafar Rezaei: Conceptualization, Formal analysis, Methodology, Supervision, Writing - Reviewing and Editing. Kateřina Staňková: Conceptualization, Formal Analysis, Funding acquisition, Methodology, Supervision, Writing- Original draft preparation, Writing- Reviewing and Editing.

Funding MS, KS, and JR are supported by European Union's Horizon 2020 research and innovation program under the Marie Skłodowska-Curie grant agreement No 955708. KS is additionally supported by the Dutch Research Council projects OCENW.KLEIN.277 and VI.Vidi.213.139.

Data Availability No datasets were generated or analysed during the current.

Declarations

Conflict of interest The authors declare no conflict of interest.

Ethical approval Not applicable.

Consent to participate Not applicable.

Consent for publication Not applicable.

References

1. Bull JW, Maron M (2016) How humans drive speciation as well as extinction. Proc R Soc B Biol Sci 283(1833):20160600
2. Hellmann J, Pfrender M (2011) Future human intervention in ecosystems and the critical role for evolutionary biology. Conserv Biol 25(6):1143–1147
3. Drumonde-Neves J, Franco-Duarte R, Lima T, Schuller D, Pais C (2016) Yeast biodiversity in vineyard environments is increased by human intervention. PLoS ONE 11(8):0160579
4. Shen X-J, Cao L-J, Chen J-C, Ma L-J, Wang J-X, Hoffmann AA, Wei S-J (2023) A comprehensive assessment of insecticide resistance mutations in source and immigrant populations of the diamondback moth Plutella xylostella (l.). Pest Manag Sci 79(2):569–583
5. Rex Consortium (2013) Heterogeneity of selection and the evolution of resistance. Trends Ecol Evol. 28(2):110–118
6. Tabashnik B, Brévault T, Carriere Y (2013) Insect resistance to bt crops: lessons from the first billion acres. Nat Biotechnol 31:510–21
7. Cunningham JJ (2019) A call for integrated metastatic management. Nature Ecol Evol 3(7):996–998
8. Brown JS, Staňková K (2017) Game theory as a conceptual framework for managing insect pests. Curr Opin Insect Sci 21:26–32
9. Conlin PL, Chandler JR, Kerr B (2014) Games of life and death: antibiotic resistance and production through the lense of evolutionary game theory. Curr Opin Microbiol 21:35–44
10. Brown JS, Parman AO (1993) Consequences of size-selective harvesting as an evolutionary game. In: The Exploitation of Evolving Resources: Proceedings of an International Conference, Held at Jülich, Germany, September 3–5, 1991, Springer, pp 248–261
11. Salvioli M, Dubbeldam J, Staňková K, Brown JS (2021) Fisheries management as a Stackelberg evolutionary game: finding an evolutionarily enlightened strategy. PLoS ONE 16(1):0245255
12. Gatenby RA (2009) A change of strategy in the war on cancer. Nature 459(7246):508
13. Staňková K, Brown JS, Dalton WS, Gatenby RA (2019) Optimizing cancer treatment using game theory: a review. JAMA Oncol 5(1):96–103
14. Bregni M, Badoglio M, Pedrazzoli P, Lanza F (2016) Is allogeneic transplant for solid tumors still alive? Bone Marrow Transpl 51:751–752
15. Al Hamed R, Bazarbachi A, Malard F, Harousseau J-L, Mohty M (2019) Current status of autologous stem cell transplantation for multiple myeloma. Blood Cancer J 9:44
16. Fernandez HF, Sun Z, Yao X, Litzow MR, Luger SM, Paietta EM, Racevskis J, Dewald GW, Ketterling RP, Bennett JM, Rowe JM, Lazarus HM, Tallman MS (2009) Anthracycline dose intensification in acute myeloid leukemia. N Engl J Med 361(13):1249–1259
17. Gatenby RA, Brown JS, Vincent T (2009) Lessons from applied ecology: cancer control using an evolutionary double bind. Cancer Res 69(19):7499–7502
18. Fardisi M, Gondhalekar AD, Ashbrook AR, Scharf ME (2019) Rapid evolutionary responses to insecticide resistance management interventions by the german cockroach (blattella germanica. l.). Sci Rep 9(1):1–10
19. Kleshnina M, Streipert S, Brown JS, Staňková K (2023) Game theory for managing evolving systems: Challenges and opportunities of including vector-valued strategies and life-history traits. Dyn Games Appl 13(4):1130–1155
20. Stein A, Salvioli M, Garjani H, Dubbeldam J, Viossat Y, Brown JS, Staňková K (2023) Stackelberg evolutionary game theory: how to manage evolving systems. Philos Trans R Soc B 378(1876):20210495
21. Martin RB, Fisher ME, Minchin RF, Teo KL (1992) Optimal control of tumor size used to maximize survival time when cells are resistant to chemotherapy. Math BSiosci 110(2):201–219
22. Tomlinson IP (1997) Game-theory models of interactions between tumour cells. Eur J Cancer 33(9):1495–1500
23. Wölfl B, Te Rietmole H, Salvioli M, Kaznatcheev A, Thuijsman F, Brown JS, Burgering B, Staňková K (2022) The contribution of evolutionary game theory to understanding and treating cancer. Dyn Games Appl 12(2):313–342
24. Broom M, Hadjichrysanthou C, Rychtár J (2010) Evolutionary games on graphs and the speed of the evolutionary process. Proc R Soc A Math Phys Eng Sci 466(2117):1327–1346

25. Hilbe C, Kleshnina M, Staňková K (2023) Evolutionary games and applications: Fifty years of 'the logic of animal conflict'. Dyn Games Appl 13(4):1035–1048
26. Marusyk A, Almendro V, Polyak K (2012) Intra-tumour heterogeneity: a looking glass for cancer? Nat Rev Cancer 12(5):323–334
27. Merlo LM, Pepper JW, Reid BJ, Maley CC (2006) Cancer as an evolutionary and ecological process. Nat Rev Cancer 6(12):924–935
28. Greaves M, Maley CC (2012) Clonal evolution in cancer. Nature 481(7381):306–313
29. Gatenby R, Brown JS (2018) The evolution and ecology of resistance in cancer therapy. Cold Spring Harb Perspect Med 8(3):033415
30. Michor F, Iwasa Y, Nowak MA (2004) Dynamics of cancer progression. Nat Rev Cancer 4(3):197–205
31. Pressley M, Salvioli M, Lewis DB, Richards CL, Brown JS, Staňková K (2021) Evolutionary dynamics of treatment-induced resistance in cancer informs understanding of rapid evolution in natural systems. Front Ecol Evol 9:460
32. Vincent TL, Brown JS (2005) Evolutionary Game Theory, Natural Selection, and Darwinian Dynamics. Cambridge University Press, Cambridge
33. Apaloo J (1997) Revisiting strategic models of evolution: the concept of neighborhood invader strategies. Theor Popul Biol 52(1):71–77
34. Apaloo J, Brown JS, Vincent TL (2009) Evolutionary game theory: Ess, convergence stability, and nis. Evol Ecol Res 11(4):489–515
35. Fisher RA (1930) The Genetical Theory of Natural Selection. Clarendon Press, Oxford
36. Metz JAJ, Geritz SA, Meszéna G, Jacobs FJ, Van Heerwaarden JS (1995) Adaptive dynamics: a geometrical study of the consequences of nearly faithful reproduction. Stochastic and Spatial Structures of Dynamical Systems, Proceedings of the Royal Dutch Academy of Science (KNAW Verhandelingen), North Holland, Amsterdam, 183–231
37. Metz JAJ, Staňková K, Johansson J (2016) The canonical equation of adaptive dynamics for life histories: from fitness-returns to selection gradients and pontryagin's maximum principle. J Math Biol 72:1125–1152
38. Cressman R, Song J-W, Zhang B-Y, Tao Y (2012) Cooperation and evolutionary dynamics in the public goods game with institutional incentives. J Theor Biol 299:144–151
39. Gallaher JA, Enriquez-Navas PM, Luddy KA, Gatenby RA, Anderson AR (2018) Spatial heterogeneity and evolutionary dynamics modulate time to recurrence in continuous and adaptive cancer therapies. Cancer Res 78(8):2127–2139
40. Jensen NF, Stenvang J, Beck MK, Hanáková B, Belling KC, Do KN, Viuff B, Nygård SB, Gupta R, Rasmussen MH et al (2015) Establishment and characterization of models of chemotherapy resistance in colorectal cancer: towards a predictive signature of chemoresistance. Mol Oncol 9(6):1169–1185
41. Carrere C (2017) Optimization of an in vitro chemotherapy to avoid resistant tumours. J Theor Biol 413:24–33
42. Khalil HK (2002) Nonlinear Systems. Prentice Hall, Saddle River
43. Dervieux A, Thomasset F (1980) A finite element method for the simulation of a Rayleigh–Taylor instability. Approximation Methods for Navier–Stokes Problems. Springer, New York, pp 145–158
44. Yuan G, Li Y (2019) Estimation of the regions of attraction for autonomous nonlinear systems. Trans Inst Meas Control 41(1):97–106
45. Mitchell IM (2008) The flexible, extensible and efficient toolbox of level set methods. J Sci Comput 35:300–329
46. Williams J (1971) Stability in noncooperative games. Oper Res 19(3):774–783
47. Vermeulen AJ (1996) Stability in non-cooperative game theory. In: PhD thesis, Nijmegen: Nijmegen Institute for Cognition and Information
48. Zhen J, Ma Z (2002) Stability for a competitive Lotka-Volterra system with delays. Nonlinear Anal Theory Methods Appl 51(7):1131–1142
49. Guo C, Fang S (2016) Stability and approximate analytic solutions of the fractional Lotka-Volterra equations for three competitors. Adv Differ Equ 2016:1–14
50. Ramazi P, Cao M (2014) Stability analysis for replicator dynamics of evolutionary snowdrift games. In: 53rd IEEE Conference on Decision and Control, IEEE, pp 4515–4520
51. Cressman R, Tao Y (2014) The replicator equation and other game dynamics. Proceedings of the National Academy of Sciences 111(supplement_3), 10810–10817
52. Bomze IM, Pötscher BM (2013) Game Theoretical Foundations of Evolutionary Stability, vol 324. Springer, Berlin
53. Apaloo J, Brown JS, McNickle GG, Vincent TL, Vincent TL (2015) Ess versus nash: solving evolutionary games. Evol Ecol Res 16(4):293–314

54. Accinelli E, Carrera EJS (2011) Evolutionarily stable strategies and replicator dynamics in asymmetric two-population games. Dynamics. Games and Science I: DYNA 2008, in Honor of Maurício Peixoto and David Rand, University of Minho, Braga, Portugal, September 8–12, 2008. Springer, Berlin, Germany, pp 25–35
55. Goh BS (1977) Global stability in many-species systems. Am Nat 111(977):135–143
56. Mougi A (2013) Allelopathic adaptation can cause competitive coexistence. Thyroid Res 6(2):165–171
57. Kim E, Brown JS, Eroglu Z, Anderson AR (2021) Adaptive therapy for metastatic melanoma: predictions from patient calibrated mathematical models. Cancers 13(4):823
58. Viossat Y, Noble R (2021) A theoretical analysis of tumour containment. Nature Ecol Evol 5(6):826–835
59. Alvarez FE, Viossat Y (2024) Tumor containment: a more general mathematical analysis. J Math Biol 88(4):41
60. Carrère C, Zidani H (2020) Stability and reachability analysis for a controlled heterogeneous population of cells. Optim Control Appl Methods 41(5):1678–1704
61. Zhang J, Cunningham JJ, Brown JS, Gatenby RA (2017) Integrating evolutionary dynamics into treatment of metastatic castrate-resistant prostate cancer. Nat Commun 8(1):1816
62. Strobl MA, West J, Viossat Y, Damaghi M, Robertson-Tessi M, Brown JS, Gatenby RA, Maini PK, Anderson AR (2021) Turnover modulates the need for a cost of resistance in adaptive therapy. Cancer Res 81(4):1135–1147
63. Bayer P, Brown JS, Staňková K (2018) A two-phenotype model of immune evasion by cancer cells. J Theor Biol 455:191–204
64. Gluzman M, Scott JG, Vladimirsky A (2020) Optimizing adaptive cancer therapy: dynamic programming and evolutionary game theory. Proc R Soc B 287:20192454
65. Bayer P, West J (2023) Games and the treatment convexity of cancer. Dyn Games Appl 13:1088–1105
66. Ardévol Martinez V, Ghaffari Laleh N, Salvioli M, Thuijsman F, Cavill R, Kather JN, Staňková K (2021) Modelling treatment of metastatic non-smallcell lung cancer through evolutionary game theory. Under review, 2127–2139
67. Staňková K, Brown JS, Dalton WS, Gatenby RA (2019) Optimizing cancer treatment using game theory: a review. JAMA Oncol 5(1):96–103
68. Bukkuri A, Pienta KJ, Amend SR, Austin RH, Hammarlund EU, Brown JS (2023) The contribution of evolvability to the eco-evolutionary dynamics of competing species. Ecol Evol 13(10):10591
69. Adaptive ChemoTherapy for Ovarian Cancer in Patients With Replased Platinum-sensitive High Grade Serous or High Grade Endometrioid Ovarian Cancer (ACTOv). https://clinicaltrials.gov/study/NCT05080556#contacts-and-locations. Accessed 17 July 2024
70. Basanta D, Gatenby RA, Anderson AR (2012) Exploiting evolution to treat drug resistance: combination therapy and the double bind. Mol Pharm 9(4):914–921
71. Gatenby RA, Zhang J, Brown JS (2019) First strike-second strike strategies in metastatic cancer: lessons from the evolutionary dynamics of extinction. Cancer Res 79(13):3174–3177
72. West JB, Dinh MN, Brown JS, Zhang J, Anderson AR, Gatenby RA (2019) Multidrug cancer therapy in metastatic castrate-resistant prostate cancer: an evolution-based strategy. Clin Cancer Res 25:4413
73. West J, You L, Zhang J, Gatenby RA, Brown JS, Newton PK, Anderson AR (2020) Towards multidrug adaptive therapy. Cancer Res 80(7):1578–1589
74. Luddy KA, West J, Robertson-Tessi M, Desai B, Burrsell TM, Barrett S, O'Sullivan J, Marignol L, Gatenby R, Brown JS et al (2024) Evolutionary double-bind treatment using radiotherapy and nk cell-based immunotherapy in prostate cancer. bioRxiv, 2024–03
75. Ghaffari Laleh N, Loeffler CML, Grajek J, Staňková K, Pearson AT, Muti HS, Trautwein C, Enderling H, Poleszczuk J, Kather JN (2022) Classical mathematical models for prediction of response to chemotherapy and immunotherapy. PLoS Comput Biol 18(2):1–18
76. Kaznatcheev A, Peacock J, Basanta D, Marusyk A, Scott JG (2019) Fibroblasts and alectinib switch the evolutionary games played by non-small cell lung cancer. Nature Ecol Evol 3:450–456
77. Soboleva A, Kaznatcheev A, Cavill R, Schneider K, Staňková K (2024) Validation of polymorphic Gompertzian model of cancer through in vitro and in vivo data. PLOS ONE, in print
78. Alix-Panabières C, Pantel K (2021) Liquid biopsy: from discovery to clinical application. Cancer Discov 11(4):858–873
79. Crowley E, Di Nicolantonio F, Loupakis F, Bardelli A (2013) Liquid biopsy: monitoring cancer-genetics in the blood. Nat Rev Clin Oncol 10(8):472–484
80. Palmirotta R, Lovero D, Cafforio P, Felici C, Mannavola F, Pellè E, Quaresmini D, Tucci M, Silvestris F (2018) Liquid biopsy of cancer: a multimodal diagnostic tool in clinical oncology. Therapeutic Adv Med Oncol 10:1758835918794630

81. Catalona WJ, Smith DS, Ratliff TL, Dodds KM, Coplen DE, Yuan JJ, Petros JA, Andriole GL (1991) Measurement of prostate-specific antigen in serum as a screening test for prostate cancer. N Engl J Med 324(17):1156–1161
82. Cunningham JJ, Gatenby RA, Brown JS (2011) Evolutionary dynamics in cancer therapy. Mol Pharm 8(6):2094–2100
83. Cunningham JJ, Brown JS, Gatenby RA, Staňková K (2018) Optimal control to develop therapeutic strategies for metastatic castrate resistant prostate cancer. J Theor Biol 459:67–78
84. Cunningham JJ, Thuijsman F, Peeters R, Viossat Y, Brown JS, Gatenby RA, Staňková K (2020) Optimal control to reach eco-evolutionary stability in metastatic castrate resistant prostate cancer. PLoS ONE 15(12):1–24
85. Karev G (2023) On the scope of applicability of the models of Darwinian dynamics. Preprint at arXiv:2302.11438
86. Lion S, Sasaki A, Boots M (2023) Extending eco-evolutionary theory with oligomorphic dynamics. Ecol Lett 26:22–46
87. Murrell DJ, Dieckmann U, Law R (2004) On moment closures for population dynamics in continuous space. J Theor Biol 229(3):421–432